PERGAMON

Energy Conversion & Management 41 (2000) 37–48

ENERGY CONVERSION & MANAGEMENT

www.elsevier.com/locate/enconman

Thermodynamic analysis of the absorption refrigeration system with geothermal energy: an experimental study

Abdullah Keçeciler, H. İbrahim Acar*, Ayla Doğan

Department of Mechanical Engineering, Faculty of Engineering, Cumhuriyet University, 58140, Sivas, Turkey

Received 12 August 1998; accepted 22 March 1999

Abstract

In the present study, an absorption refrigeration system, which is alternative to the ordinary mechanical refrigeration system, is designed. For this purpose, an experiment using geothermal energy in the Hot Spring in Sivas is set up in the lab conditions, and a thermodynamic analysis of the Absorption Refrigeration System (ARS) operating on water–lithium bromide is performed. The change in the coefficient of performance of the ARS has been graphically investigated with the various parameters and the results are tabulated. These results show that geothermal energy in the Hot Spring in Sivas cannot be used efficiently in electricity generation. However, taking into account the need of storing at 4–10°C, this geothermal resource can be used especially for refrigeration, and it will provide a considerable economical gain. © 1999 Elsevier Science Ltd. All rights reserved.

Keywords: Refrigeration; Geothermal; Absorption

1. Introduction

Absorption Refrigeration Systems (ARSs) become economically attractive when there is a source of inexpensive heat energy at a temperature of 50–200°C. Some examples of inexpensive heat energy sources include geothermal energy, solar energy and waste heat from cogeneration or process steam plants, that is, heat energy that otherwise would be wasted.

* Corresponding author. Fax: +90-346-2261-545.
E-mail address: iacar@cumhuriyet.edu.tr (H.İ. Acar)

PII: S0196-8904(99)00091-6

Nomenclature

COP	coefficient of performance
ARS	absorption refrigeration system
f	circulation ratio
h	specific enthalpy (kJ/kg)
m	mass flow rate (kg/s)
P	pressure (Pa)
T	temperature (K)
X	mass concentration (kg LiBr/kg Solution)
η	effectiveness
Q	heat flow (kW)
Δ	difference
W	Work

Subscripts

ab	absorber
co	condenser
ev	evaporator
ge	generator
o	state of surroundings
f	weak solution
z	rich solution
w	work
k	loss
p	pump

ARSs involve the absorption of a refrigerant by a transport medium. The most widely used ARS is the ammonia–water system, where ammonia (NH_3) serves as the refrigerant and water (H_2O) as the transport medium. Other ARSs include water–lithium chloride and water–lithium bromide systems, where water serves as the refrigerant.

In the present study, the lithium–bromide system, which uses geothermal energy, was designed in lab conditions with the aim of refrigeration. As shown in Fig. 1, the ARS looks very much like the vapour compression system, except that the compressor has been replaced by a complex absorption mechanism consisting of an absorber, a pump, a generator, a heat exchanger and a valve. Once the pressure of the H_2O is raised by the components in the absorption mechanism, it is cooled and condensed in the condenser by rejecting heat to the surroundings, throttled to the evaporator pressure and receives heat from the refrigerated space as it flows through the evaporator.

The water vapour leaves the evaporator and enters the absorber, where it chemically reacts with the lithium bromide to form $H_2O{\cdot}LiBr$. This is an exothermic reaction, thus heat is released during this process. The amount of H_2O that can be dissolved in LiBr is inversely

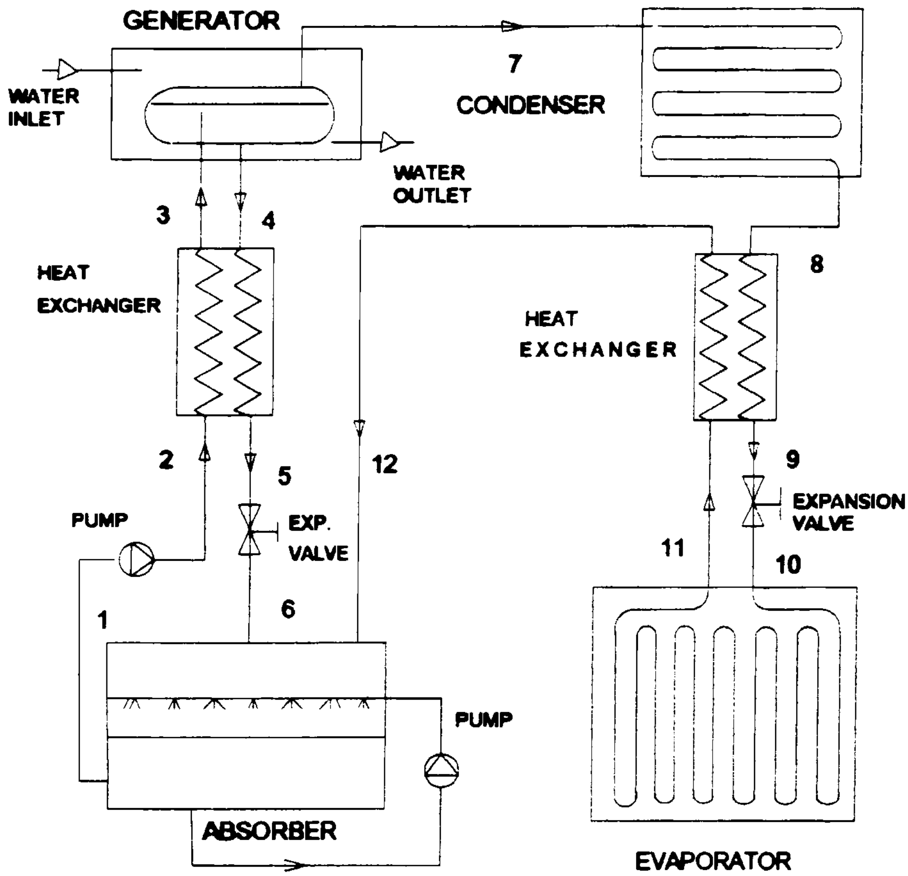

Fig. 1. Schematic diagram for the cycle.

proportional to the temperature. Therefore, it is necessary to cool the absorber to maintain its temperature as low as possible, hence, to maximise the amount of H_2O dissolved in the LiBr. The liquid H_2O + LiBr solution, which is rich in H_2O, is then pumped to the generator. Heat is transferred to the solution from a suitable source to vaporise some of the solution. The high pressure pure H_2O vapour then continues its journey through the rest of the cycle. The hot H_2O + LiBr solution, which is weak in H_2O, then passes through a heat exchanger, where it transfers some heat to the rich solution leaving the pump and is throttled to the absorber pressure (Fig. 1).

Compared with vapour compression systems, ARSs have one major advantage: a liquid is compressed instead of a vapour. The steady flow work is proportional to the specific volume, and thus, the work input for the ARS is very small and often neglected in the cycle analysis. The operation of this system is based on heat transfer from an external source. Therefore, ARSs are often classified as heat driven systems [1]. These systems are not without disadvantages. They are bulky, complex and, of course, expensive. However, they are economically competitive when there is an available source of energy that would otherwise be wasted. They are generally used in industrial applications.

Geothermal energy, which has high potential, is attractive for the refrigeration system as the low temperature heat energy source. Since the mechanical compression systems require a large amount of electrical energy, the ARS, using geothermal energy, is one of the strongest alternatives. The cooling effect can be obtained with different chemical, physical and electrical processes in the ARS. The steady state closed loop cycle or open loop cycle can be used for this system.

1.1. Geothermal resource

Turkey is the seventh country in the world with respect to geothermal resources. There are 140 geothermal fields whose temperature exceeds 40°C in Turkey [2]. One of them is the Hot Spring in Sivas where geothermal water is approximately at a temperature of 50°C, and its volume flow rate, obtained without any loss, is 500 l/s.

Fig. 2 shows the existing hot water sources and water pipe network in the Hot Spring. As shown in Fig. 2, 1–2: DMRET (Directorate of the Mineral Resource and Exploration of Turkey) camp, 3: DMRET drilling well, 4–5: open pools, 6: big closed pool, 7–8: A and B baths, 9: C bath and general WC, 10: D and E baths, 11: new hotel, 12: F and G baths, 13: drilling well, 14: drilling well, and 15: station of measuring volume flow rate (Fig. 2).

Three drilling processes have been performed so far. In 1976, the first drilling was performed by DMRET up to 240.70 m deep, and the hot water obtained in the depth of 158–209 m was at 46.5°C and 45 l/s volume flow rate. The second drilling process was performed in 1984. Although the hot water was seen at 178 m deep, the blow-out process was performed at 184 m, wherein the hot water obtained was at 60°C and 417 l/s. In 1986, the third drilling process was performed, and the hot water obtained at 172 m deep was at 60°C [3].

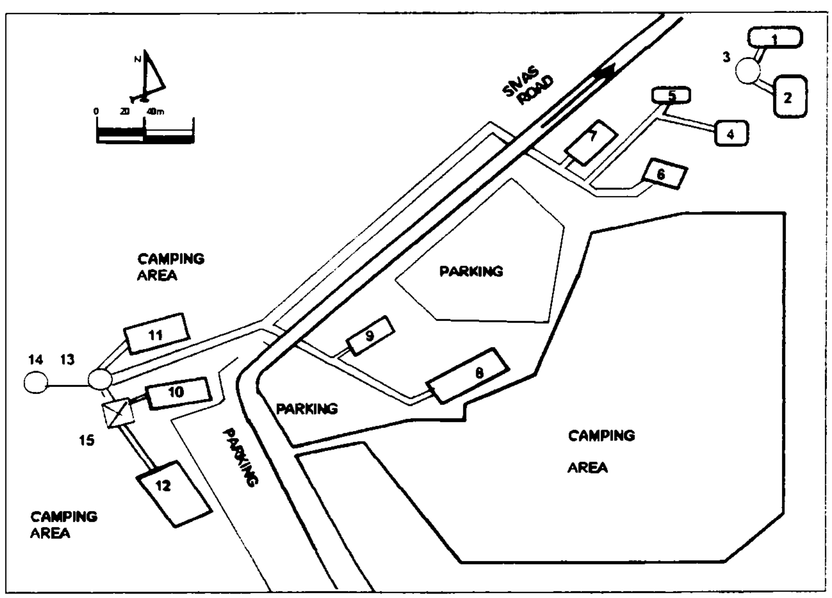

Fig. 2. A general view of the Hot Spring.

1.2. Chemical properties of the geothermal water

The geothermal water in the Hot Spring is included in the 'very hot water' category [3] and in the group of bicarbonate water, which has a weak radioactivity [4]. Its electrical conductivity and total hardness are 2000–3250 μs/cm and 62.5–94.5 mg/l $CaCO_3$, respectively. Its pH values are between 7.32 and 7.52. It contains much more dissolved substance than 1 g/l.

2. Thermodynamic analysis of the system

As shown in Fig. 1, the ARS essentially consists of an evaporator, generator, condenser and absorber. The temperatures of the condenser, generator, evaporator and absorber are the basic working temperatures. When the ARS is considered to operate on the ideal Carnot refrigeration cycle, the thermodynamic relations used in the analysis of the system are as follows:

$$\Delta Q + W = \Delta U \tag{1}$$

$$\Delta S = \frac{\Delta Q}{T} + \frac{W_{\mathrm{k}}}{T_0} \tag{2}$$

ΔU and ΔS are equal to zero, since the refrigeration system is the closed loop system. If the pump work is neglected, the first and second laws of thermodynamics give [5,6],

$$Q_{\mathrm{ev}} + Q_{\mathrm{ge}} + Q_{\mathrm{co}} + Q_{\mathrm{ab}} = 0 \tag{3}$$

$$\frac{Q_{\mathrm{ev}}}{T_{\mathrm{ev}}} + \frac{Q_{\mathrm{ge}}}{T_{\mathrm{ge}}} + \frac{Q_{\mathrm{co}}}{T_{\mathrm{co}}} + \frac{Q_{\mathrm{ab}}}{T_{\mathrm{ab}}} + \frac{W_{\mathrm{k}}}{T_0} = 0 \tag{4}$$

The ARS can be regarded as the combination of a mechanical vapour compression system and a heat pump system. The entropy decrease in the condenser is equal to the entropy increase in the evaporator for reversible processes [7]. Thus, the following equation is written

$$\frac{Q_{\mathrm{ev}}}{T_{\mathrm{ev}}} = \frac{Q_{\mathrm{co}}}{T_{\mathrm{co}}} \tag{5}$$

Since the loss work is equal to zero for an ideal cycle, from Eqs. (4) and (5),

$$\frac{Q_{\mathrm{ge}}}{T_{\mathrm{ge}}} = \frac{Q_{\mathrm{ab}}}{T_{\mathrm{ab}}} \tag{6}$$

2.1. COP of the reversible ARS

The thermodynamic efficiency of the ARS is evaluated by means of the coefficient of performance (COP), which is [8],

$$\mathrm{COP} = \frac{Q_{\mathrm{ev}}}{Q_{\mathrm{ge}}} \tag{7}$$

The loss work is equal to zero for a reversible ideal cycle. Hence, if Eqs. (3) and (4) are rearranged,

$$\frac{Q_{\mathrm{ev}}}{Q_{\mathrm{ge}}} + \frac{Q_{\mathrm{co}}}{Q_{\mathrm{ge}}} + \frac{Q_{\mathrm{ab}}}{Q_{\mathrm{ge}}} = 0 \tag{8}$$

$$\frac{Q_{\mathrm{ev}}}{Q_{\mathrm{ge}}}\frac{T_{\mathrm{ge}}}{T_{\mathrm{ev}}} + \frac{Q_{\mathrm{co}}}{Q_{\mathrm{ge}}}\frac{T_{\mathrm{ge}}}{T_{\mathrm{co}}} + \frac{Q_{\mathrm{ab}}}{Q_{\mathrm{ge}}}\frac{T_{\mathrm{ge}}}{T_{\mathrm{ab}}} = 0 \tag{9}$$

If Eqs. (5), (6), (8) and (9) are introduced into Eq. (7),

$$\mathrm{COP} = \frac{T_{\mathrm{ev}}\left(T_{\mathrm{ge}} - T_{\mathrm{ab}}\right)}{T_{\mathrm{ge}}(T_{\mathrm{co}} - T_{\mathrm{ev}})} \tag{10}$$

It can be seen from Eq. (10) that the COP of the system essentially depends on four working temperatures, but it is not dependent on ambient conditions.

2.2. COP of the theoretical ARS

The relations between mass flow rate and heat flow rate can be written by means of the mass flow rates and the enthalpy values in the different points of the system. Thus, the following equations are obtained:

$$Q_{\mathrm{ev}} = m_7(h_{11} - h_{10}) \tag{11}$$

$$m_7 = m_8 = m_9 = m_{10} = m_{11} = m_{12} \tag{12}$$

$$m_1 = m_2 = m_3 \tag{13}$$

$$m_4 = m_5 = m_6 \tag{14}$$

$$m_1 = m_6 + m_{12} \tag{15}$$

$$m_3 = m_4 + m_7 \tag{16}$$

$$Q_{\mathrm{co}} = m_7(h_7 - h_8) \tag{17}$$

$$Q_{\mathrm{ge}} = m_7h_7 + m_4h_4 - m_3h_3 \tag{18}$$

$$Q_{\mathrm{ab}} = m_4h_6 + m_7h_{12} - m_3h_1 \tag{19}$$

The circulation ratio is defined as follows [9],

$$f = \frac{m_1}{m_7} \tag{20}$$

or

$$f = \frac{X_{ge}}{X_{ab}} = \frac{X_z}{(X_z - X_f)} \tag{21}$$

Substituting Eqs. (11), (18) and (20) into Eq. (7) gives,

$$\mathrm{COP} = \frac{(h_{11} - h_{10})}{h_7 + f(h_4 - h_3) - h_4} \tag{22}$$

As seen from Eq. (22), the major parameters which affect the COP are the latent heat of vaporisation and the circulation ratio. When $(h_{11} - h_{10})$ increases, the COP increases. When the circulation ratio increases, the COP decreases.

3. Experimental

An experiment which was built in lab conditions is shown in Fig. 3. It essentially consists of an evaporator, a generator, a condenser and an absorber, the temperatures of which are the

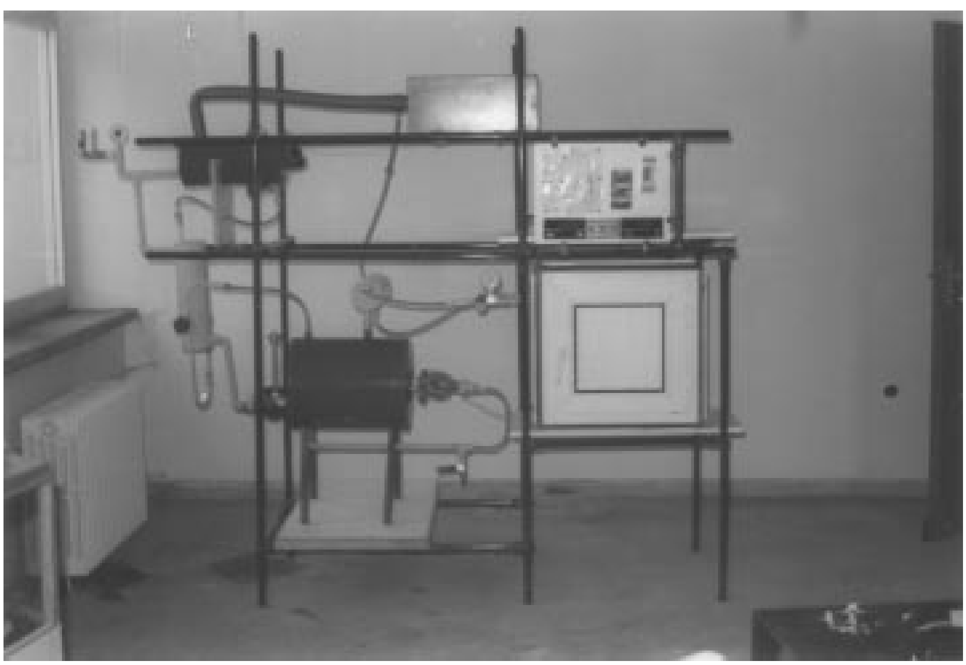

Fig. 3. A general appearance of the experimental set.

basic working temperatures (Fig. 3). Water is used as the refrigerant and lithium bromide as the transport medium. The data used in the experimental study are calculated and shown in Table 1. The relations in Ref. [8] are used for calculation of the thermodynamic properties of water–lithium bromide (Table 1).

4. Results and discussion

The thermodynamic analysis of the ARS with $LiBr/H_2O$ is performed, and the heat interaction in each component is analysed. The results obtained are preserved in the graphs and tables.

Fig. 4 shows the change in the COP with the source temperature. The COP increases as the generator temperature increases for the evaporator temperatures of 4, 6 and 8°C. This is due to the fact that the amount of vaporised refrigerant increases as the heat to the generator increases, and then the circulation ratio decreases. The decrease causes an increase in the COP because the circulation ratio and the COP value are inversely proportional.

Fig. 5 shows the change in the COP with the evaporator temperature for the different condenser temperatures. A considerable decrease in the circulation ratio has been seen at the high evaporator and low condenser temperatures. It causes a rise in the COP.

Fig. 6 shows the change in the COP with the evaporator temperature. The absorber temperature is a parameter, and the condenser and generator temperatures are constant. It is observed that the COP tends to increase at the low absorber and high evaporator temperatures. As mentioned earlier, the decrease in the circulation ratio causes this increase.

It can be seen in Fig. 7 that the COP increases at the low absorber and high generator temperatures. The amount of vaporised refrigerant increases because the generator temperature is high. Likewise, the mass concentration of the solution increases parallel to the increase in the

Table 1
Calculated thermodynamics properties of the working fluids pair

State	T (°C)	P (kPa)	X (%)	m (kg/s)	H (kJ/kg)
1	30	2.6	44	0.65	62.5
2	30.5	5.8	44	0.65	62.6
3	35.3	5.8	44	0.65	76.3
4	42	5.8	48	0.50	91.1
5	38	5.8	48	0.50	85.1
6	37	2.7	48	0.50	85.1
7	60	5.8	0	0.15	2609.7
8	20	4.6	0	0.15	83.86
9	18	4.6	0	0.15	75.5
10	17	3.2	0	0.15	75.5
11	8	2.9	0	0.15	1579.3
12	14	2.9	0	0.15	1600.3

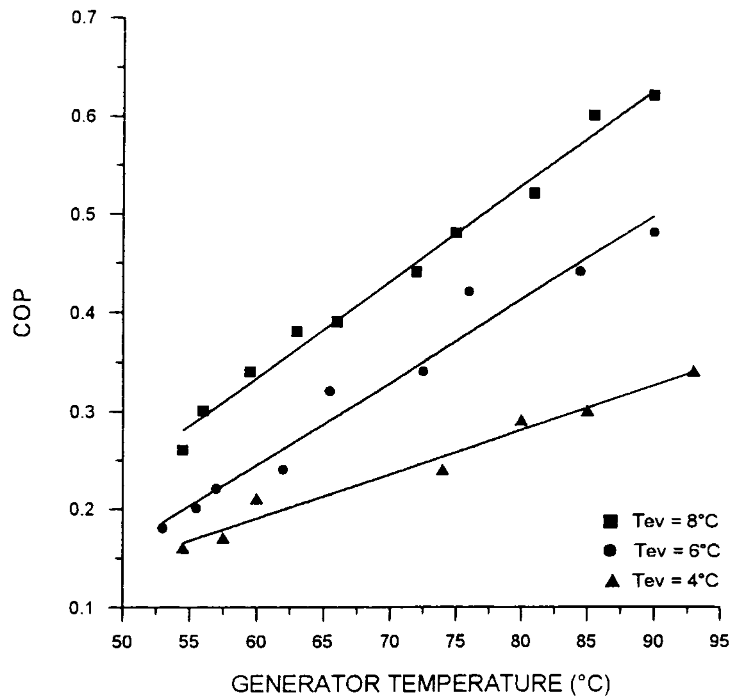

Fig. 4. The change in the COP with the generator temperature at the various evaporator temperatures.

generator temperature. Since the difference between the refrigerant and absorbent concentration rises, the circulation ratio decreases. Therefore, the COP value increases.

It is observed in Fig. 8 that the COP is high at the low condenser and absorber temperatures. Decreasing the amount of refrigerant and increasing the mass flow rate of the air to the condenser reduce the condenser temperature. The decrease in the amount of refrigerant in the condenser causes the increase in the circulation ratio as well as the decrease in the COP value. The increase in the mass flow rate of the air causes a decrease in the condenser temperature. As a result, an increase occurs in the COP (Figs. 4–8).

Table 2
Results of the experimental study

COP	0.5654
f	4.33
m_{ge} (kg/s)	12.5
η	0.80
Q_{ge} (kW)	387.41
Q_{co} (kW)	378.87
Q_{ev} (kW)	225.57
Q_{ab} (kW)	241
W_p (kW)	0.01

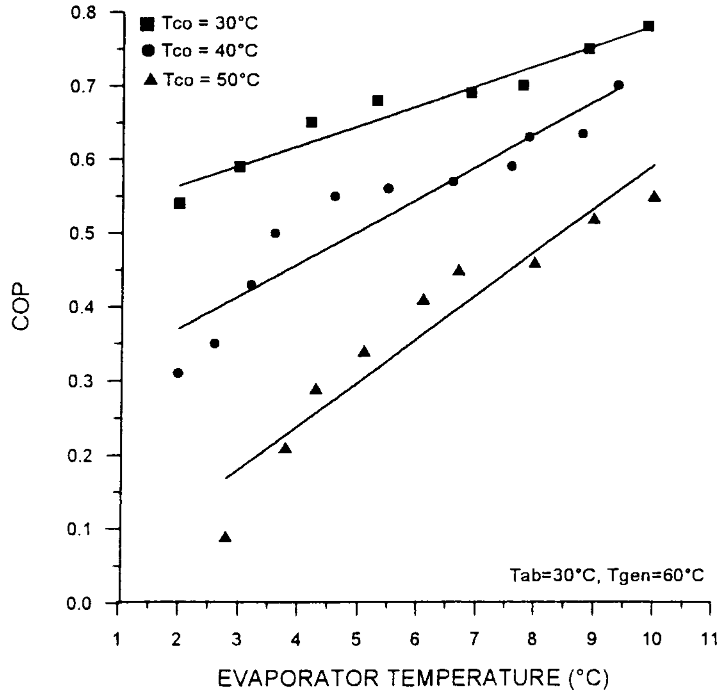

Fig. 5. The change in the COP with the evaporator temperature at the various condenser temperatures.

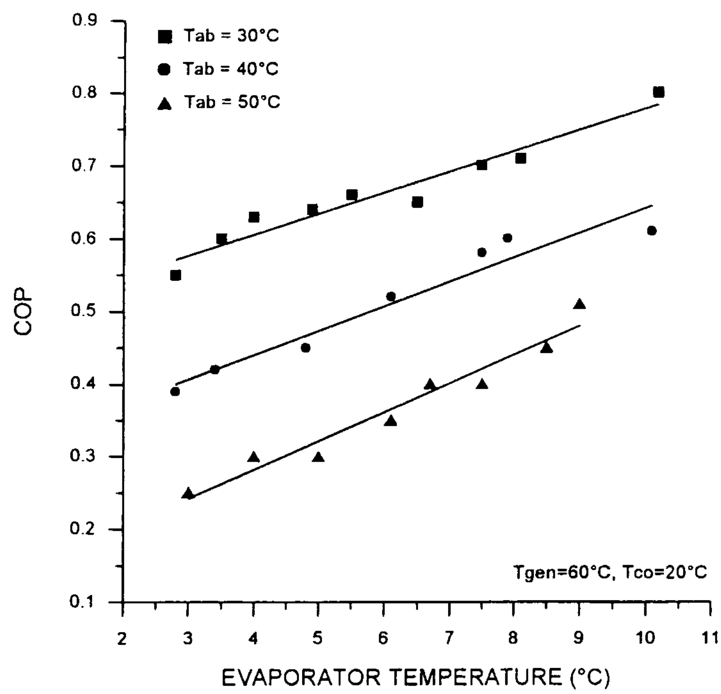

Fig. 6. The change in the COP with the evaporator temperature at the various absorber temperatures.

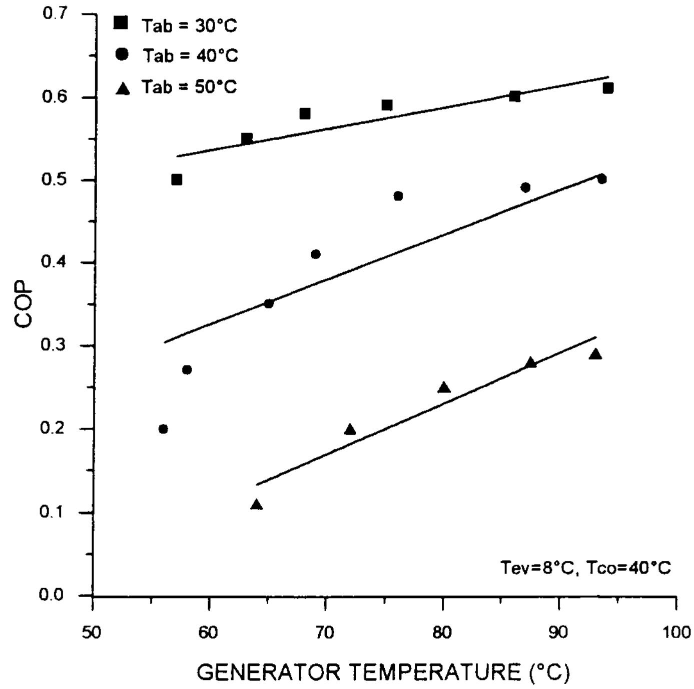

Fig. 7. The change in the COP with the generator temperature at the various absorber temperatures.

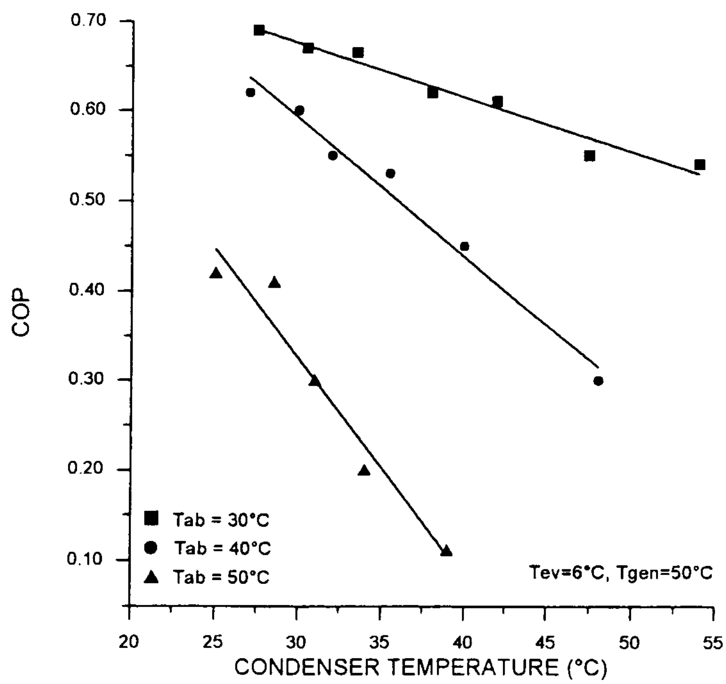

Fig. 8. The change in the COP with the condenser temperature at the various absorber temperatures.

5. Conclusions

The results obtained show that the mass flow rate of 12.5 kg/s from the geothermal source at 60°C is sufficient for about 225.57 kW cooling effect (see Table 2). When the mass concentrations, of the strong and weak solutions in the generator and absorber are 44 and 48%, respectively, the maximum COP is obtained. The evaporator temperature drops to 2–3°C in the best conditions, which is provided by keeping the absorber temperature at 30–35°C. For this reason, this cooling method can be used only with the aim of storing fruits and vegetables at 4–10°C, as well as air conditioning. In addition, if the geothermal energy resource in the Hot Spring in Sivas is used for refrigeration, it will provide a considerable economic gain.

References

[1] Eisa MAR, Rashed IGA, Devotta S, Holland FA. Applied Energy 1986;25:71.
[2] Mertoğlu O. Orme Jeotermal 1992;2:10.
[3] Ergin C. Sicak Çermik Yöresinin Jeolojisi ve Jeolojik Enerji Olanaklari. Cumhuriyet University Publication, Sivas, 1992, p. 15.
[4] Çağlar KÖ. Türkiye Maden Sulari ve Kaplicalari. Directorate of the Mineral Resource and Exploration of Turkey Publication, Ankara, 1961, p. 639.
[5] Eisa MAR, Devotta S, Holland FA. Applied Energy 1986;24:287.
[6] McNeelly LA. ASHRAE Trans 1979;85:413.
[7] Kumar P, Devotta S. ASHRAE Trans 1990;96:291.
[8] Felli M. Absorption Refrigeration Thermodynamics 1991;97:189–204.
[9] Eisa MAR, Devotta S, Holland FA. Applied Energy 1986;24:287.